Journal of Visualization, Vol. 10, No. 2 (2007)227-235

Regular Paper

Visualization and Force Measurement of High-Temperature, Supersonic Impulse Jet Impinging on Baffle Plate

Mizukaki, T.*

* The First Research Center, Technical Research and Development Institute, Japan Defense Agency, Naka-Meguro, Meguro, Tokyo, 153-8630, Japan. (Current affiliation: Dept. of Aeronautics and Astronautics, School of Engineering, Tokai University, 1117, Kitakaname, Hiratsuka, Kanagawa, 259-1292 Japan) E-mail: mizukaki@keyaki.cc.u-tokai.ac.jp

Received 20 September 2006
Revised 2 February 2007

Abstract : The flow visualization and force measurement of a supersonic impinging jet on a center-holed vertical baffle plate were investigated. Center-holed baffle plates of 2d to 5d in diameter, with a 1d center hole were tested, where d is the bore of the launch tube. The standoff distance of the baffle plates from the open end of the launch tube were varied to be from 2d to 5d. The supersonic impulse jet, with an incident shock wave of Mach 2.89 was produced by a high-enthalpy blast-wave simulator. The direction-indicating color schlieren method produced a two-dimensional density gradient of the flow field around the baffle plate. In addition, the flow fields were numerically analyzed, using two-dimensional asymmetric Euler equations. The results of the numerically-analyzed and the experimentally-visualized flow field agreed well. The visualized flow field indicates that the baffle plate should be at least 3.5d in diameter to deflect the supersonic impinging jet at an angle greater than a right angle. We have concluded that the representative method of designing muzzle brakes for military purpose accurately predicts the force yielded by the supersonic impinging impulse jet on the vertical baffle plate only when there is a large ratio of the baffle-plate diameter to the bore of the launch tube.

Keywords : Flow visualization, Supersonic impinging jet, Blast wave, Shock tube.

1. Introduction

Shock tubes are experimental apparatus for high-speed aerodynamic research and find wide application in generating shock waves and high-speed flow in laboratories, providing test durations from hundreds of μs to ms. Both the shock waves and the induced high-speed flow are employed for research not only in aerospace engineering (Viren et al., 2005) but also into industrial issues, such as the exhaust noise generated by automobile's engines (Sekine et al., 1990). Several experiments have been carried out to evaluate the strength of noise produced by a single-stage powder gun, which assumed that the shock-wave-induced, high-speed flow generated at the open end of a shock tube behaves similar to the combustion gas emerging from the gun (Phan and Hurdle, 1990). The combustion gas emerging from a muzzle has a similar property to that of a shock-induced impulse jet, determined by the ratio of the muzzle pressure to that of the ambient environment (Addy, 1981). Applying optical flow visualization techniques, such as the schlieren method (Merzkirch, 1987) for combustion gas is unsuitable, because of the large number of unburned particles of the propellant and the flame, both of which prevent light from the light source from passing through the test section, while the high-speed impulse jet induced by a shock tube is translucent. Thus, investigating the

high-speed impulse jet emerging from shock tubes is useful in clarifying the aerodynamic characteristics of the gunpowder-combustion gas emerging from the muzzle.

When a single-stage powder gun operates, a recoil force, generated in the direction opposite the projectile launch, results from the momentum of the combustion gas expanding inside the gun barrel. The amount of propellant—gunpowder—needed to accelerate the projectile to the required velocity increases with the projectile size. Therefore, without anchoring the single-stage powder gun, the increasing recoil momentum, caused by the expanding combustion gas and the projectile motion, prevents the safe operation, or steady, and accurate projectile launching. Almost all single-stage powder guns that use large-size projectiles for military purposes are equipped with a device that reverses the direction of part of the combustion gas at the muzzle (Rheinmetall GmbH, 1982). The device used is called a *muzzle brake*. Establishing a design for a brake that can control the thrust of a high-speed impulse jet, by deflecting the part of the main flow, has potential not only for the military, but also in industry. A standard design for muzzle brake has been proposed by Soifer (Soifer, 1974), and assumes the combustion jet to be a continuous flow, which collides with the muzzle device under elastic conditions. The combustion jet emerging from the muzzle, however, is an unstable phenomenon, which includes shock waves, and contains aerodynamic structures, such as the Mach disc. Several studies have reported numerical analysis calculating the effects of the muzzle device. Most of the work has been performed on a particular and complex shape of a unique muzzle device (Buell and Widhopf, 1984; Cooke, 1987; Cayzacr and Carette, 2000). To our knowledge, no comparison between Soifer's method and experimental results has been investigated in detail. Thus, a study comparing Soifer's method with the experimental results, obtained from a supersonic impulse jet, is needed to confirm the flexibility of Soifer's method. Since 1997, the Transitional Ballistic Simulation Facility (TBSF) has been conducting ballistics research at the Technical Research and Development Institute of Japan Defense Agency (TRDI). The TBSF can simulate the free-flight aerodynamic conditions equivalent to flight at Mach number 3, with blast waves.

This study was made to measure the force generated by the collision between vertical muzzle brake models and the supersonic impulse jet induced by the shock wave of Mach number 2.89 by using TBSF. A hydrocode AUTODYN-2D was used to analyze the flow field around the muzzle brake model. The direction-indicating color schlieren method was employed to visualize the flow field, and the resulting images were confirmed with the pressure maps of the numerical results. The interaction force predicted by Soifer's method at the vertical muzzle brake model was evaluated by both the experimental and numerical results.

2. Experimental Method

2.1 A High Enthalpy Blast Wave Simulator

The TBSF has the unique capability of allowing us to shoot a projectile downwards through a blast wave, and against a supersonic wind blown upwards. A blast-wave simulator, called the high-enthalpy blast simulator (HEBS), produced the blast waves. Figure 1 and Table 1 show a schematic diagram of HEBS and its flow characteristics, respectively. Also, Fig. 2 shows typical overpressure histories inside HEBS at P2, P3, P4, P5, and P6. In Fig. 2, time $t = 0$ indicates the moment when an incident shock wave arrives at P4. Although detailed descriptions are given in the references (Hisajima, 1999; Nasuno, 2003; Mizukaki and Arisawa, 2004), for convenience, a brief summary is given here.

Initially, a high pressure (2 MPa) is contained in a high-pressure chamber. When the quick valve opens, the free piston accelerates along the compression tube, producing a series of compression waves, which compress and heat the working gas. As the pressure in the compression tube builds up, the 1-mm thickness stainless steal diaphragm separating the working gas from the ambient air ruptures, releasing the working gas, which expands through the launch tube to develop a supersonic, high-enthalpy flow in the test section.

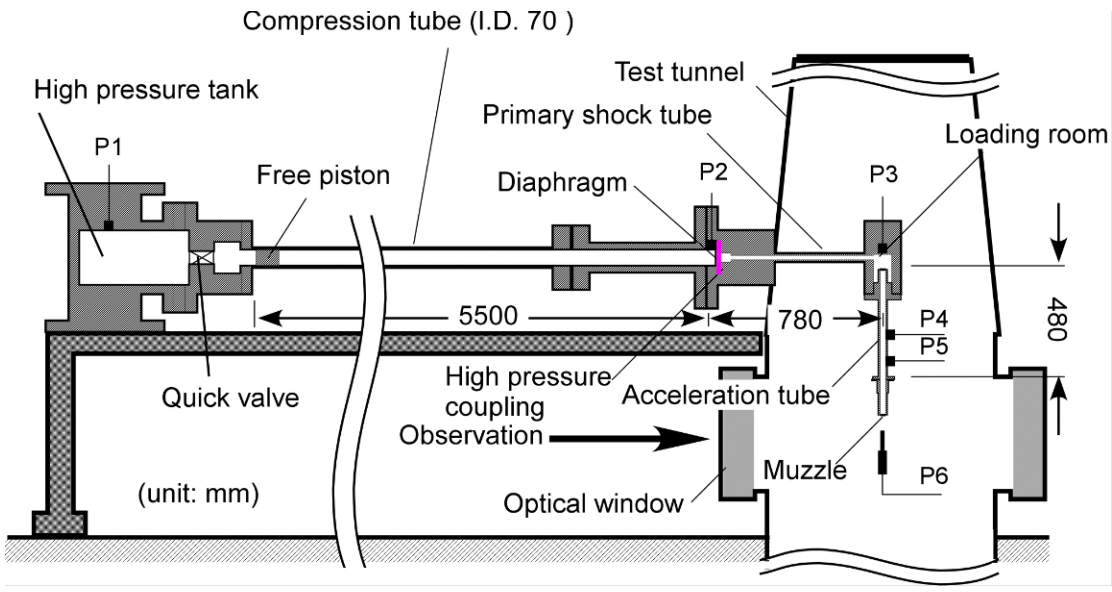

Fig. 1. Schematic diagram of the High-Enthalpy Blast-Wave Simulator (HEBS), P: pressure transducer.

Table 1. The characteristics of supersonic-impulse jet generated by HEBS.

Flow	Properties		
Incident Shock Wave	Mach number	Ms	2.89
Test gas	Velocity	u_1	0 m/s
	Pressure	p_1	0.101
	Temperatu	T_1	288 K
Hot gas	Velocity	u_2	721 m/s
	Pressure	p_2	0.958
	Temperatu	T_2	735 K
	Mach	M_2	1.33
	Duration	δt	1 ms

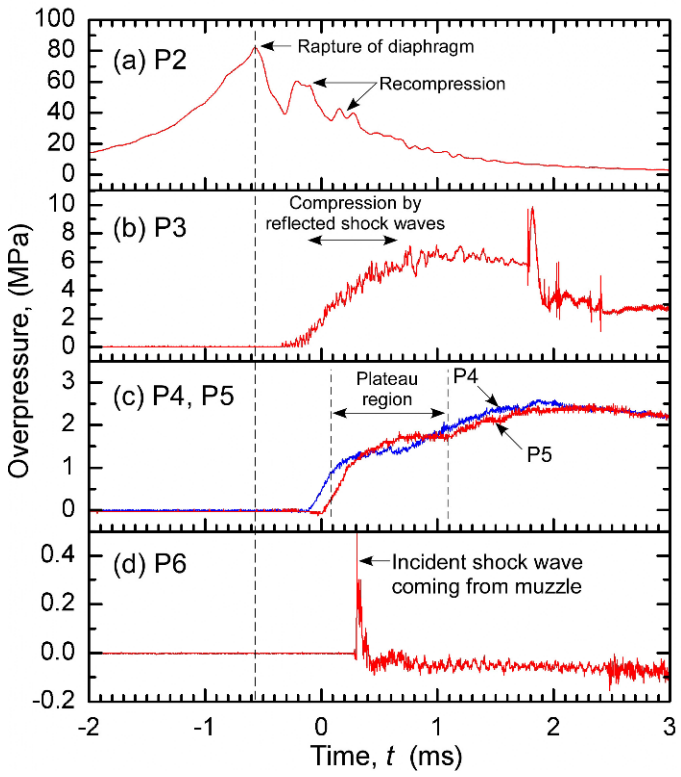

Fig. 2. Typical overpressure histories of HEBS.

2.2 Visualization Method

The direction-indicating, color schlieren method (DInCS) was used to visualize the density field around the muzzle. By using the DInCS, a two-dimensional density gradient generated by the pulsed jet can be revealed with color gradients in the first attempt.

Figure 3 shows the optical alignment of DInCS. Generally, images obtained by the schlieren method indicate the density gradient of the flow. The ordinary monochrome schlieren method indicates a one-dimensional density gradient. In contrast, DInCS displays a two-dimensional density gradient, using color gradient. Therefore, DInCS can measure the detailed structure of a relatively complicated flow field. A high-intensity, short-duration Xe spark light (NANO-SPARK, NS-4000P, BIOLEK) was used as the light source. Visualized images were recorded with a digital still camera with a 4024 × 1324 pixel resolution (Nikon D1x). The literature (Kleine and Grönig, 1991) indicates DInCS in detail.

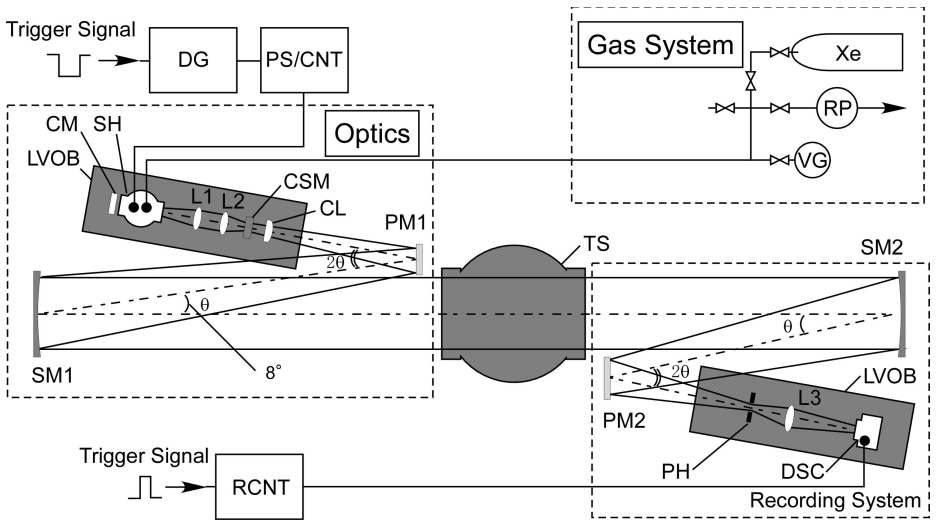

Fig. 3. Schematic diagram of optical visualization set-up for DInCS: DG: Digital delay generator, PS/CNT: Power supply, SH: Spark head, CM: Concave mirror, L: Lens, CSM: Color source mask, CL: Cylindrical mirror, PM: Parabolic mirror, SM: Schlieren mirror, TS: Test section, PH: Pine hole, DSC: Digital steal camera, (unit: mm).

2.3 Muzzle-Brake Model

Figure 3 shows the muzzle brake model used in this experiment. The launch tube was modified, as shown in Fig. 3, to measure the forward force exerted on the baffle plate. The model was a simplified muzzle brake, found on typical artillery. By concentrating the compression force generated between flange-A and B, by a collision of the jet against the baffle plate, the forward force was presumably verified. Flexible tubing connected the model with the launch tube. Four PZT-load cells (upper frequency limit: 75 kHz, resolution: 0.045 N rms, Type-200B series, PCB piezotronics Inc.) were used to verify the generated force. The cells were arranged at a right angle on flange-B. The bore of the launch tube, made of SUS-304, was of a 25-mm thick diameter. To measure the temperature of the jet, the tube was equipped with a co-axial, short-response, thermocouple (3 μs rise time). Circular baffle plates with a 25-mm diameter center hole, for passing the projectile, were tested. The maximum diameter and standoff distance from the open end was D/d = 5, X/d = 5, respectively, where D/d and X/d are non-dimensional distances, scaled by d.

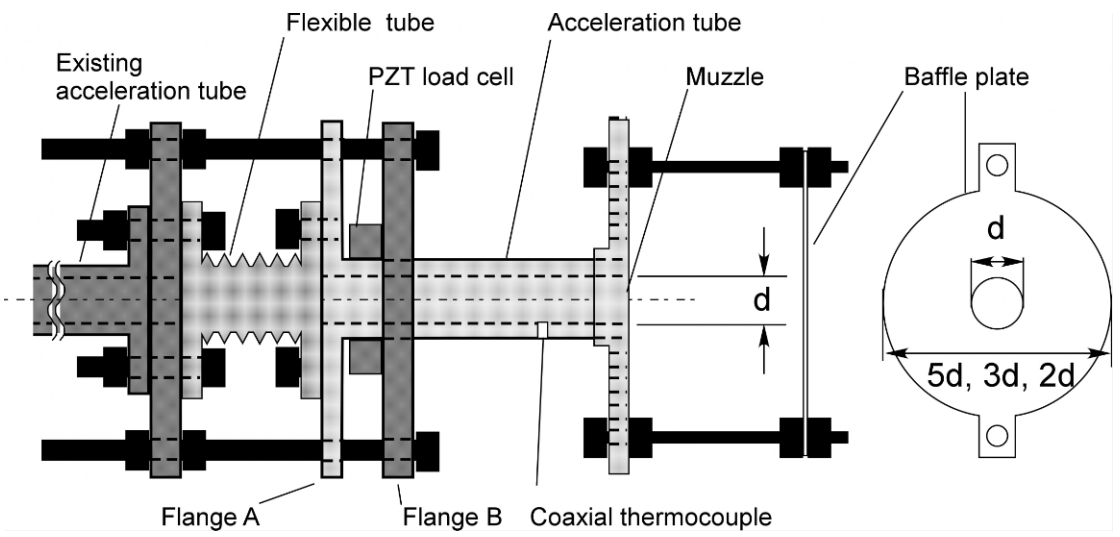

Fig. 4. Schematic diagram of the muzzle brake model for forward force measurement and flow visualization.

2.4 Numerical Simulation

For the theoretical interpretation of the experimental results, numerical simulations were performed by a commercial hydrocode, ATODYN-2D (Century Dynamics, 1997), on an SGI workstation at the Computation Center of TRDI. The Euler equations of an axially symmetric pulsed flow were solved by a finite difference, flux-corrected transport (FCT)-scheme. The computation domain is shown in Fig. 5 and the mesh number is 250 by 150. On the outer boundary and downstream boundary, the ambient gas condition is applied: $(p, \rho, u, v) = (p_1, \rho_1, 0, 0)$, where ρ is the gas density, u the axial velocity, and v the radial velocity of the gas flow. On the walls of the muzzle brake model, the baffle plate, and the jet axis, the symmetric condition is applied. On the upstream boundary inside the shock tube, the shock condition $(p, \rho, u, v) = (p_2, \rho_2, 0, 0)$ is applied, where the quantities denoted by the subscript 2 are obtained through the Rankine-Hugoniot relations for $M = 2.89$. The shock condition $M = 2.89$ was continued for 1 ms according to the experimental result shown in Fig. 2(c). The duration with stable pressure is indicated as "Plateau region". Corresponding to the experiments, the radius, and the standoff distance from the open end of the launch tube, of the baffle plate was set to be equal to the individual condition performed in the experiment. The force generated by supersonic impinging jet on the baffle plate examined was evaluated by summing up the momentum provided by the jet. For force computation, we did not take the deformation of a baffle plate by impinging jet into account by assuming that the baffle plate examined was a rigid body.

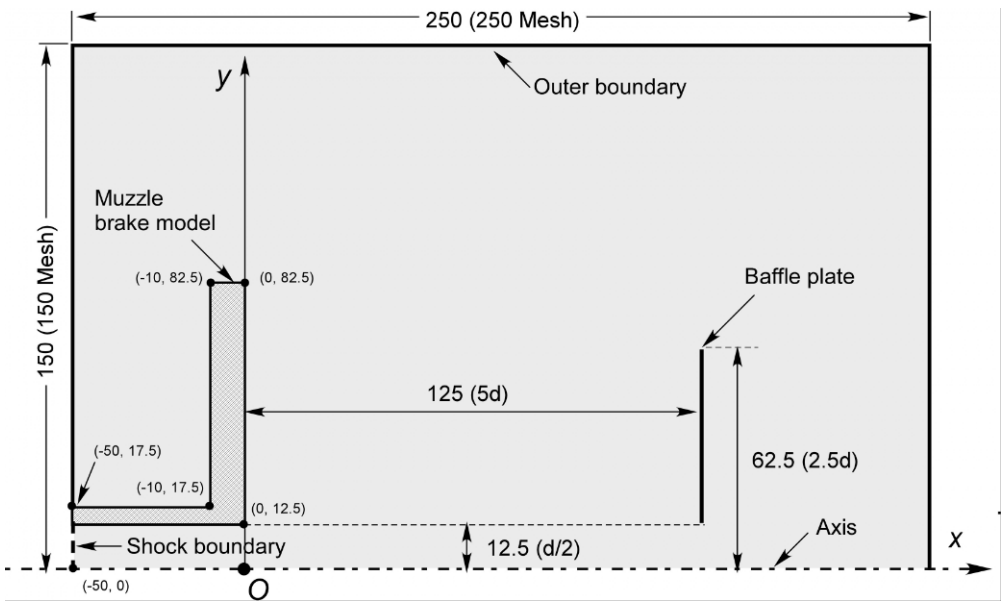

Fig. 5. Computational domain for the flow field analysis for D/d = 5, X/d = 5.

3. Results and Discussion

The flow field comparison is made with figures presented in Fig. 6, where experimentally-visualized images (on the lower half) from each baffle location are compared with numerically-analyzed density contours (on the upper half). The arrangement of the apparatus in both fields is shown in Fig. 6(a). In the upper half of the figure, one can see the support pillar, but it is not visible in the lower half. The reproduction of the support pillar in the computational domain was not made, since we assumed that the support pillar had a negligible effect on the flow field. It should be noted that the center hole of the baffle cannot be seen on the images, as they represent a side view. The typical flow field between muzzle and baffle plate is shown in Fig. 6(b). The flow field comparison for each layout of the baffle plate, D/d = 2, 3, and 5, are shown in Fig. 6(c), 6(d), and 6(e), respectively, after the incident shock waves (Ms = 2.89) emerged from the open end of the launch tube. The density increments of the

contours of Fig. 6(c), 6(d), and 6(e) indicate 5 % of the initial density. In the case of D/d = 5, baffle plate was slightly bent by supersonic impinging jet, as shown in Fig. 6(e). The bent plate was replaced before next shot every time so that the affect of bending to the deflection direction of jet was minimized. We assumed that the bending occurred was not large deformation enough to affect the flow properties around the model. We assumed that both the shape and the location of the Mach disk (indicated as MD) and the deflected jet (indicated as red arrow) agree in the DInCS images and the computational results from AUTODYN-2D. However, there is no quantitative information on the density field, where the deflected jet and the vortex ring, generated by the jet, impinge on the baffle plate. This is because the schlieren method integrates the density divergence along the optical path length in the test section. With respect to force measurement, actual force was measured by PZT-load cells equipped with main body of muzzle brake model as shown in Fig. 4. Therefore, we did not assume that small deformation of a baffle plate by impinging jet gave a significant affection for the results of force measurement. Both the computational results by AUTODYN-2D and the experimental imaging indicate that the emerging direction of the deflected jet depends heavily on the layout of the baffle plate. Now we focus on the emerging direction of the jet, deflected by the baffle plate. We define the deflection angle of the deflected jet, θ_{def}, as the angle between the axis of the launch tube, and the emerging direction. The deflection-angle map, obtained by the visualized images, is presented in Fig. 7. The data, except those obtained from the visualized images, were interpolated by the Lagrange method. We assume that the baffle plate can efficiently generate forward force when the deflection angle is more than a right angle. The deflection-angle map indicates that the diameter ratio of the baffle plate to the launch tube bore, D/d, must be greater than 3.5 to deflect the emerging impulse jet away from the axis of the launch tube at more than a right angle.

The historical forward-force data, determined by both the sensors equipped with the muzzle brake model and the numerical analysis with AUTODYN-2D, are shown in Fig. 8. The results were given by: D/d = 5 and X/d = 3. The ordinate is the forward force indicated by an arbitrary unit. The abscissa is the time elapsed from the point that an incident shock wave discharged from the open end of the launch tube. The forward force signals, collected by the sensors, were processed with a low-pass filter to remove the noise produced by the facility's mechanical vibration. The signals separately indicated the forces arising from both the hot and cold gas. We considered that numerical results from AUTODYN-2D contain oscillations due to the effects of numerical oscillation. Here, we defined the force value as the maximum forward force: F_{max}, at the time when the signal reached a peak after the cold gas' arrival. Now we focus on the F_{max} of both the experimental and numerical results. All of the experimental F_{max} values, as well as those obtained by numerical analysis with AUTODYN-2D, and by Soifer's method, are plotted against the X/d in Fig. 9. The ordinate is the normalized maximum forward force, NF_{max}, which is verticalized by the value of the NF_{max} obtained at the baffle-plate layout of X/d = 5, D/d = 3 for each method. As shown in Fig. 9, the experimental data agree well with the computational results from AUTODYN-2D. The maximum difference between experimental and numerical results NF_{max} was less than 5% for all the conditions examined here. The value of the NF_{max}, however, determined by Soifer's method did not agree with those of other methods, except for the layout at D/d = 5. We think that Soifer's method (the quasi-steady theory) could not predict the force produced by the baffle plate of medium diameter ratio because its assumptions would not evaluate the force generated the supersonic impulse jet.

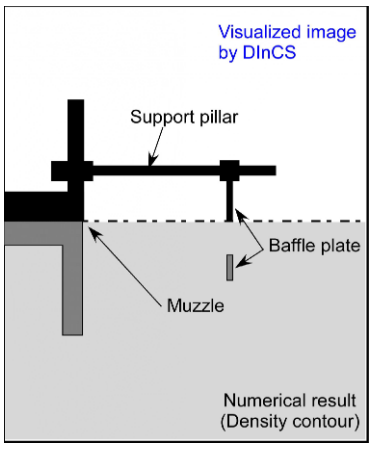

(a) Common layout of images

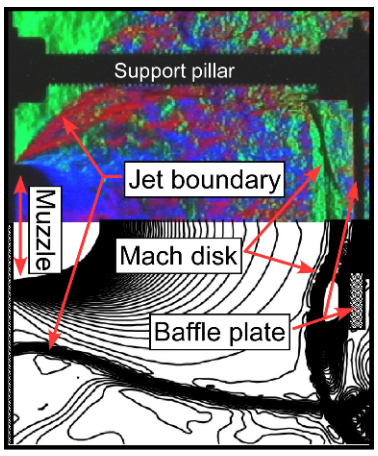

(b)Typical flow field between muzzle and baffle plate

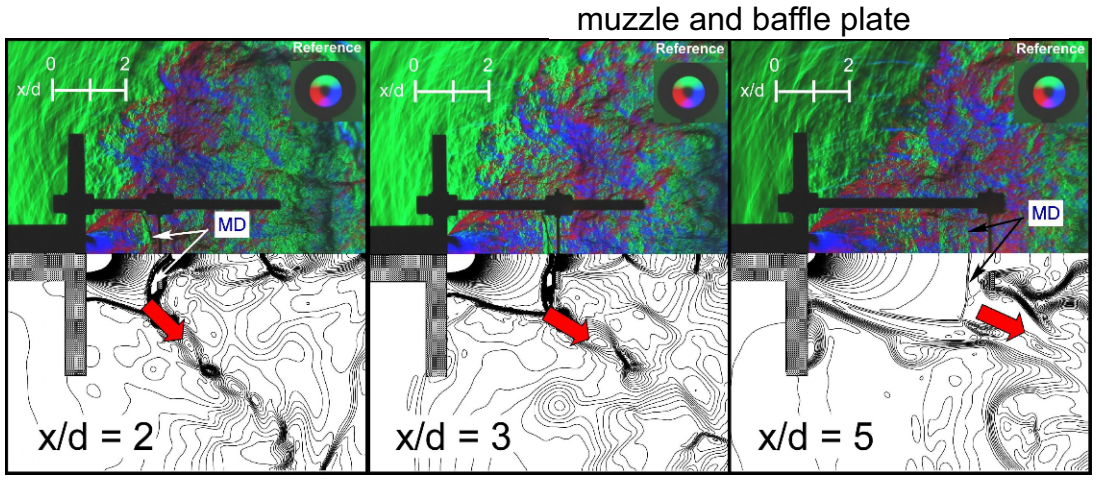

(c) D/d = 2

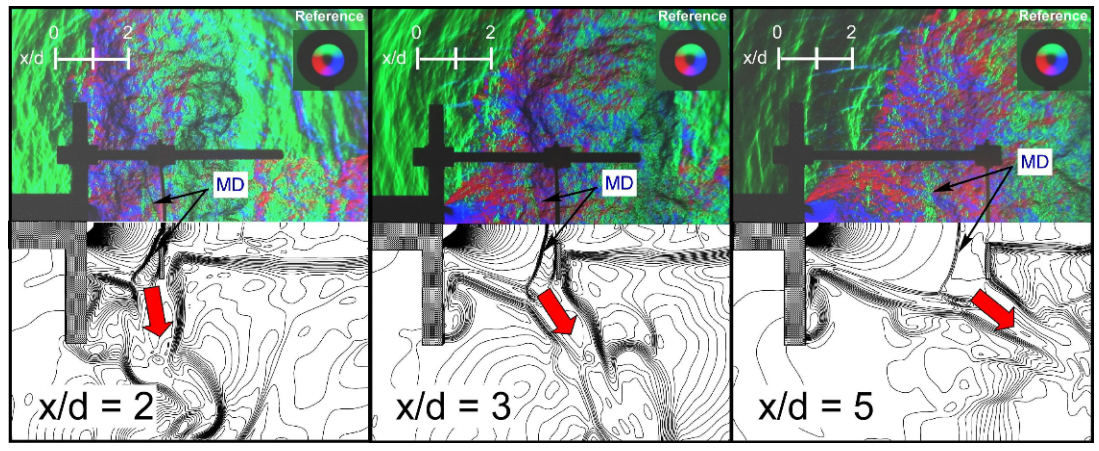

(d) D/d = 3

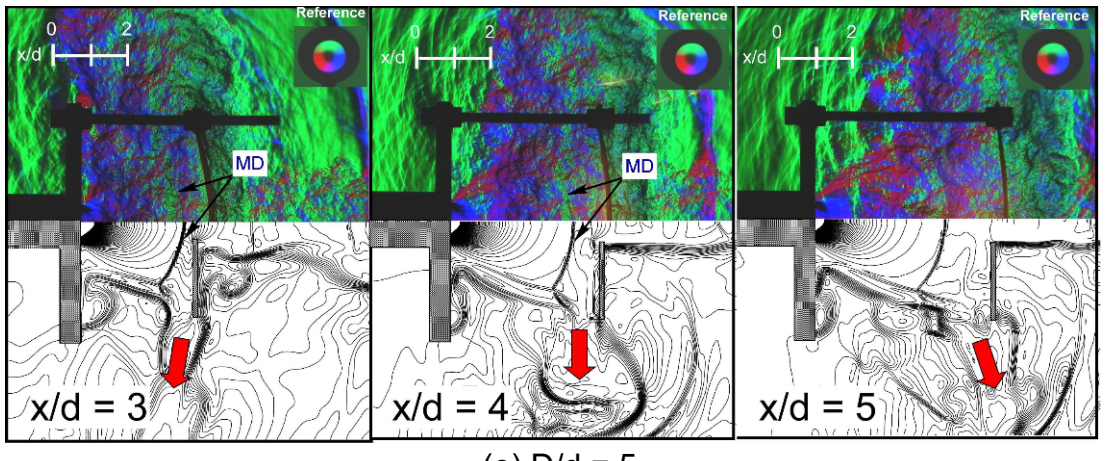

(e) D/d = 5

Fig. 6. Visualized flow field and numerical results around the vertical center-holed baffle plate at t = 1 ms; Red arrows: the deflection of the deflected jet, MD: Mach disk.

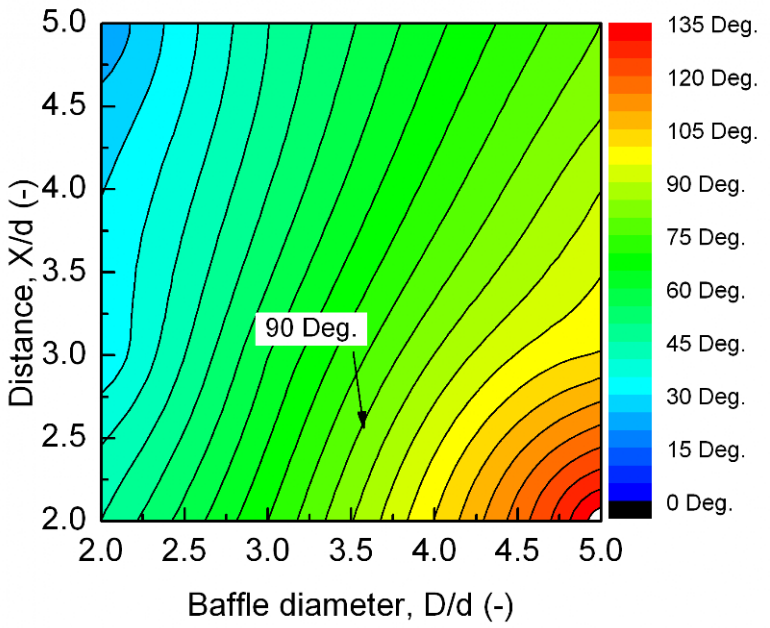

Fig. 7. The deflection angle θ_{def} map.

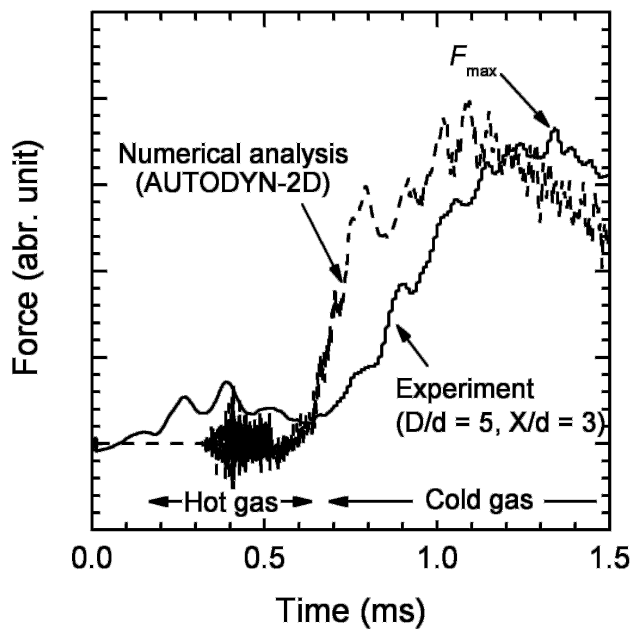

Fig. 8. An example of experimental and numerical history of the forward force.

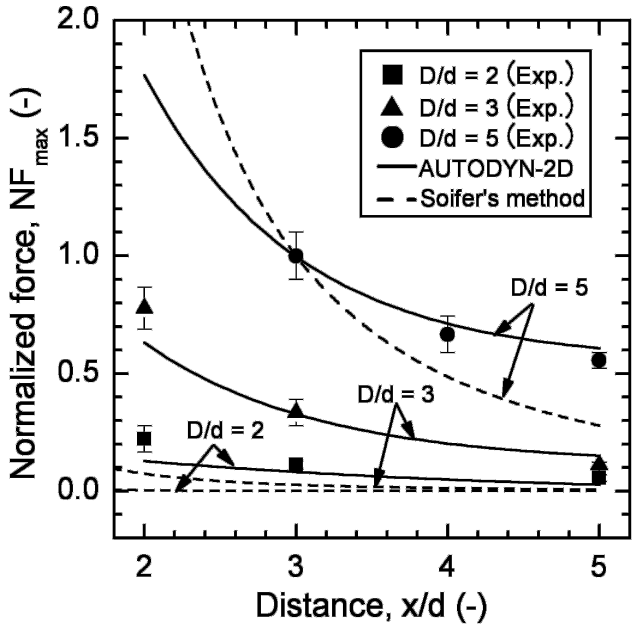

Fig. 9. The comparison of the normalized forward force.

4. Conclusions

This study used a supersonic impulse jet, generated by a high-enthalpy, blast-wave simulator to investigate the interaction between the supersonic impulse jet and a center-holed baffle plate to confirm the representative design method for the muzzle brake. The results obtained are as follows:

(1) Direction-indicating color schlieren method clearly visualizes the complex flow field of the supersonic impinging jet around the baffle plate.
(2) Measurements using PZT load cells clearly detected the forward force generated by both the hot gas and the cold gas.
(3) Using the representative design method for a muzzle brake for military use, we obtained reasonable results of the forward force generated by a baffle plate of D/d = 5 in diameter, but not of a baffle plate of D/d = 2 and 3. Therefore, the representative design method is not suitable for

designing muzzle brakes with small diameter ratio.

(4) A ratio of baffle diameter to the bore of the launch tube of more than 3.5 is required to deflect a supersonic jet emerging from the muzzle at more than a right angle at the baffle plate.

(5) We have shown the possibility for development of a high-efficiency middle-ratio (e.g., D/d = 3) muzzle brake using the new design method.

(6) Future work is needed to investigate the interaction between a muzzle brake model that uses multiple baffle plates and the emerging supersonic jet during a projectile launch.

References

Addy, A. L., Effects of axisymmetric sonic nozzle geometry on Mach disk characteristics, AIAA Journal, 19-1 (1981), 121-122.

Buell, J. C. and Widhopf, G. F., Three-dimensional simulation of muzzle brake flowfields, AIAA Paper 84-1641, AIAA 17th Fluid Dynamics, Plasma Dynamics, and Lasers Conference (Snowmass, Colorado), (1984).

Cayzacr, R. and Carette, E., Intermediate ballistic and aeroballistics overview and perspectives, European Forum on Ballistic of Projectiles (Saint-Louis, France), (2000).

Century Dynamics, AUTODYN electronic document Library, (1997), Century Dynamics.

Cooke, C. H., Application of an explicit TVD scheme for unsteady, axisymmetric, muzzle brake flow, International Journal for Numerical Methods in Fluids, 7 (1987), 621-633.

Hisajima, S., Outline of transition ballistic simulation facility, Defense Technology Journal, 19-6 (1999), 4-12.

Kleine, H. and Grönig, H., Color schlieren methods in shock wave research, Shock Waves, 1 (1991), 51-63.

Merzkirch, W., Flow visualization, (1987), Academic Press.

Mizukaki, T. and Arisawa, H., Visualization of gun muzzle blast wave using direction-indicating color schlieren method, Technical Report No. 6852, Technical Research and Development Institute, Japan Defense Agency, (2004).

Nasuno, Y., Study on transitional ballistic simulation technology, Defense Technology Journal, 23-6 (2003), 24-31.

Phan, K. C. and Hurdle, C. V., Blast wave investigation using a high enthalpy blast simulator, Shock Waves and Tubes (ed. Y. W. Kim), (1990), 903-908, American Institute of Physics.

Rheinmetall GmbH, Handbook on Weaponry, (1982), Rheinmetall GmbH, Düsseldorf.

Sekine, N., Matsumura, S., Aoki, K. and Takayama, K., Generation and propagation of shock waves in the exhaust pipe of a 4 cycle automobile engine, Shock Waves and Tubes (ed. Y. W. Kim), (1990), 903-908, American Institute of Physics.

Soifer, M. T., Muzzle brake analysis, Technical Report WVT-CR-74010, S & D Dynamics, Inc., (1974).

Viren, M., Jagadeesh, G., Reddy, K. P. J., Sun, M. and Takayama, K., Visualization of shock waves around hypersonic spike blunt cones using electric discharge, Journal of Visualization, 8-1 (2005), 65-72.

Author Profile

Toshiharu Mizukaki: He received his B.Sc. (Sc) in Physics in 1991 from Tokyo University of Science. Form 1991 to 1999, he worked in Japan Atomic Energy Agency (JAEA) as a scientist. He received his Ph.D. in Aerospace Engineering in 2001 from Tohoku University. He worked at NASA Langley Research Center as a visiting scientist in 2001, in Technical Research and Development Institute of Japan Defense Agency from 2002 to 2005, and in Department of Aerospace Engineering of Indian Institute of Science in 2005. He has been working in Department of Aeronautics and Astronautics, School of Engineering, Tokai University, as an associate professor since 2006. His research interests are Shock Waves, High-Speed Launch System, Flow Visualization, and Laser-applied measurement Techniques.